J. Fluid Mech. (2019), *vol.* 861, *pp.* 517–523. © Cambridge University Press 2019
doi:10.1017/jfm.2018.926

Fourfold amplification of solitary-wave Mach reflection at a vertical wall

Jeffrey Knowles[1] **and Harry Yeh**[1,†]

[1]School of Civil and Construction Engineering, Oregon State University, Corvallis, OR 97331, USA

(Received 15 May 2018; revised 16 July 2018; accepted 13 November 2018;
first published online 3 January 2019)

With the use of a higher-order Euler formulation, we numerically study the reflection of an obliquely incident solitary wave at a vertical wall and compare results with the higher-order Kadomtsev–Petviashvili theory. A maximum amplification of 3.91 is achieved along the wall, nearly realizing the fourfold prediction by Miles (*J. Fluid Mech.*, vol. 79 (1), 1977, pp. 171–179).

Key words: shallow water flows, solitary waves, surface gravity waves

1. Background

The first explorative laboratory work on the reflection of solitary waves with oblique incidence along a vertical wall was reported by Perroud (1957). Perroud observed a wave configuration resembling the 'Mach reflection' pattern (see figure 1) originally attributed to compressible shockwaves (von Neumann 1943). Inspired by Perroud's experimental findings, Miles (1977*a*,*b*) developed a theory considering a shallow-but-finite water depth and small-but-finite wave amplitude to the lowest order. His theory predicts a maximum amplification of $\alpha_w = a_M/a_i = 4$ at the wall when $\psi_i = \sqrt{3a_i}$ for a small angle of incidence ψ_i. Here, the parameter a_M is the maximum amplitude at the wall and a_i is the incident wave amplitude. All lengths are normalized by the still water depth h_0 and time is normalized by $\sqrt{g/h_0}$, where g is the gravitational acceleration. Melville (1980) conducted laboratory experiments in an attempt to validate Miles's theory, but only attained an amplification of 2.0 at the wall. Funakoshi (1980) conducted numerical experiments, but only achieved a maximum amplification of $\alpha_w \approx 3.42$. Unlike Funakoshi (1980), whose numerical model was of the same order of approximation as the theory by Miles (1977*a*,*b*), Tanaka (1993) conducted numerical experiments based on a higher-order pseudo-spectral method to solve the Euler formulation. This higher-order model allowed Tanaka to study conditions less restricted by ψ_i and a_i. However, this model only yielded an amplification of $\alpha_w = 2.897$.

The theoretical prediction of a fourfold amplification of the Mach stem can also be arrived at through Kadomtsev–Petviashvili (KP) theory as shown by Chakravarty & Kodama (2009), and corresponds to the confluence of the so called (3142)-type and (2143)-type solutions. Miles (1977*b*) introduced the interaction parameter $k = \psi_i/\sqrt{3a_i}$

† Email address for correspondence: harry@oregonstate.edu

https://doi.org/10.1017/jfm.2018.926 Published online by Cambridge University Press

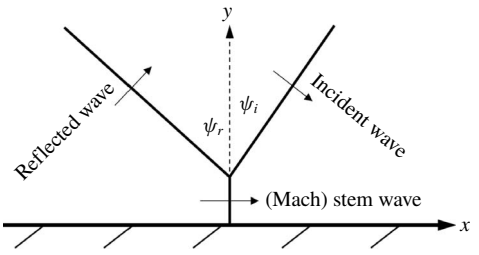


FIGURE 1. Mach reflection: ψ_i, incident wave angle; ψ_r, reflected wave angle.

in order to predict wave amplification. Based on the KP theory, Li, Yeh & Kodama (2011) heuristically proposed the following modification:

$$k = \frac{\tan\psi_i}{\sqrt{3a_i}\cos\psi_i}. \tag{1.1}$$

To achieve a consistent theory, a normal form of the KP equation with higher-order corrections was derived by Kodama & Yeh (2016) resulting in

$$k = \frac{\sqrt{1+\sqrt{1+5a_i}}\tan\psi_i}{\sqrt{6a_i}\cos\psi_i}, \tag{1.2}$$

together with the newly defined KP amplification

$$\hat{\alpha} = \begin{cases} \dfrac{\alpha_w(1+\sqrt{1+5a_i})}{(1+\sqrt{1+5\alpha_w a_i})\cos^2\psi_i}, & \text{for } k<1, \\ \alpha_w, & \text{for } k>1, \end{cases} \tag{1.3}$$

where

$$\alpha_w = \begin{cases} (1+k)^2, & \text{for } k<1, \\ \dfrac{4}{1+\sqrt{1-k^{-2}}}, & \text{for } k>1. \end{cases} \tag{1.4}$$

Equation (1.3) can be used to convert data to the KP coordinate which produces a better agreement between experimental and theoretical results (see Kodama & Yeh 2016). Hereinafter, k will refer to (1.2). In spite of this higher-order interpretation of the wave amplification, the resulting amplifications for both numerical and laboratory experiments are still $\hat{\alpha} \approx 3$. Here we revisit this remarkable prediction of the fourfold amplification by following the same procedure as Tanaka (1993), but with the use of better computational capabilities available nowadays.

2. Numerical methodology

A higher-order pseudo-spectral method developed by Dommermuth & Yue (1987) is used to simulate the reflection of an obliquely incident solitary wave at a vertical wall, which is practically the same model as that used by Tanaka (1993) and Jia (2014). The Zakharov–Craig–Sulem formulation (Zakharov 1968; Craig & Sulem 1993) of the full

https://doi.org/10.1017/jfm.2018.926 Published online by Cambridge University Press

water-wave equations is solved numerically:

$$\left.\begin{array}{ll} \Phi_{xx}+\Phi_{yy}+\Phi_{zz}=0 & \text{for } -1\leqslant z\leqslant \eta,\\ \Phi_z=0 & \text{at } z=-1,\\ \left.\begin{array}{l}\eta_t+\nabla\Phi^S\cdot\nabla\eta-(1+|\nabla\eta|^2)\Phi_z=0\\ \Phi^S_t+\eta+\frac{1}{2}|\nabla\Phi^S|^2-\frac{1}{2}(1+|\nabla\eta|^2)\Phi_z^2=0\end{array}\right\} & \text{at } z=\eta, \end{array}\right\} \tag{2.1}$$

where $\Phi(\boldsymbol{x}, z, t)$ is the velocity potential, $\eta(\boldsymbol{x}, t)$ is the surface displacement, $\Phi^S(\boldsymbol{x}, t)=\Phi(\boldsymbol{x}, z=\eta(\boldsymbol{x}, t), t)$ is the velocity potential at the free surface, $\nabla=(\partial/\partial x, \partial/\partial y)$ represents the horizontal gradient and $\boldsymbol{x}=(x, y)$. The velocity potential is expressed as a series expansion:

$$\Phi(\boldsymbol{x}, z=\eta, t)=\Phi^S(x, y, t)=\sum_{m=1}^{M}\sum_{k=0}^{M-m}\epsilon^m\frac{\eta^k}{k!}\left.\frac{\partial^k\phi^{(m)}}{\partial z^k}\right|_{(\boldsymbol{x},z=0,t)}. \tag{2.2}$$

Here $\epsilon\ll 1$ and

$$\phi^{(m)}(\boldsymbol{x}, z, t)=\sum_{p=-\infty}^{\infty}\sum_{q=-\infty}^{\infty}\phi^{(m)}_{p,q}(t)\frac{\cosh|\boldsymbol{k}_{p,q}|(z+1)}{\cosh(|\boldsymbol{k}_{p,q}|)}\mathrm{e}^{\mathrm{i}\boldsymbol{k}_{p,q}\cdot\boldsymbol{x}}. \tag{2.3}$$

The basis functions $\phi^{(m)}$ satisfy Laplace's equation as well as the bottom kinematic boundary condition. In (2.3) $\boldsymbol{k}_{p,q}=(p\pi/L_x, q\pi/L_y)$ is the wave number vector, where L_x and L_y are the length and width of the domain, respectively, $\mathrm{i}=\sqrt{-1}$, and the sum is truncated at some large $N\sim O(1000)$.

A four-stage Runge–Kutta (RK4) method (e.g. Boyce & DiPrima 2009) is used to numerically time-integrate the evolution equations:

$$\left.\begin{array}{l}\eta_t=-\nabla\Phi^S\cdot\nabla\eta+(1+|\nabla\eta|^2)\Phi_z,\\ \Phi^S_t=-\eta-\frac{1}{2}|\nabla\Phi^S|^2+\frac{1}{2}(1+|\nabla\eta|^2)\Phi_z^2.\end{array}\right\} \tag{2.4}$$

The horizontal gradient is calculated by the algebraic derivative by making use of the two-dimensional fast Fourier transform (FFT2). The initial conditions for the surface displacement η and the velocity potential at the water surface Φ^S are given by the higher-order solitary wave solution (Grimshaw 1971)

$$\left.\begin{array}{rl} \eta=a_iS^2-\frac{3}{4}a_i^2(S^2-S^4)+a_i^3\left(\frac{5}{8}S^2-\frac{151}{80}S^4+\frac{101}{80}S^6\right), & \\ \Phi^S=2\sqrt{\frac{a_i}{3}}\left\{T+a_i\left[\frac{5}{24}T-\frac{1}{3}S^2T+\frac{3}{4}(1+\eta)^2S^2T\right]\right. & \\ +a_i^2\left[-\frac{1257}{3200}T+\frac{9}{200}S^2T+\frac{6}{25}S^4T+(1+\eta)^2\left(-\frac{9}{32}S^2T-\frac{3}{2}S^4T\right)\right. & \\ \left.\left.+(1+\eta)^4\left(-\frac{3}{16}S^2T-\frac{3}{2}S^4T\right)\right]\right\}. & \end{array}\right\} \tag{2.5}$$

In (2.5) S and T are

$$S=\operatorname{sech}\kappa[(x-x_i)\cos\psi_i-y\sin\psi_i], \quad T=\tanh\kappa[(x-x_i)\cos\psi_i-y\sin\psi_i], \tag{2.6a,b}$$

in which $\kappa=\sqrt{3a_i}/2(1-(5/8)a_i+(71/128)a_i^2)$ and x_i is the initial location of the crest at the vertical wall. This solution is correct up to the third order, so the perturbation expansion is also truncated at the third term ($M=3$).

https://doi.org/10.1017/jfm.2018.926 Published online by Cambridge University Press

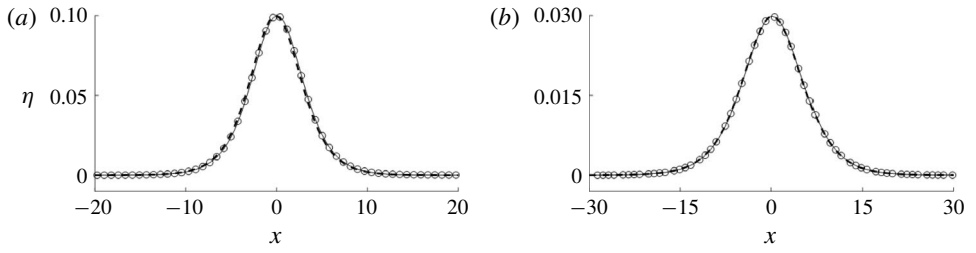


FIGURE 2. (*a*) Overlay of computed solitary wave for $a_i = 0.1$, $\psi_i = 0°$. (*b*) Overlay of computed solitary wave for $a_i = 0.03$ and $\psi_i = 15°$, where the boundary condition is treated to eliminate wave diffraction. In both plots the computed profile is presented at $t = 313.2$ (solid line), $t = 3132$ (dashed line) and $t = 6264$ (circles).

t	V	Error (%)
313.2	185.7196	−0.00022
9 396	185.72	0
21 924	185.72	0
23 490	185.7197	−0.00016

TABLE 1. Conservation of volume V for the case $a_i = 0.1$, $\psi_i = 0°$. The longest simulation time to compute the max $\hat{\alpha}$ was 157 857.

At the offshore boundary the solitary wave maintains its initial identity by artificially extending its form beyond the computational domain. This treatment allows us to achieve a long computational time by circumventing the effects of wave diffraction at the offshore boundary. To accomplish this, we use the same method implemented by Tanaka (1993) and Jia (2014).

On account of the initial conditions being a-periodic, the domain is extended periodically in the horizontal directions to accommodate for the Fourier basis functions. It takes a very large domain to run the simulation to reach the asymptotic state, causing the calculation to be quite formidable. A computer with a CPU of 3.40 GHz is used to simulate a number of trials for various combinations of a_i and ψ_i. The spatial resolution in the x and y direction is taken to be $\mathrm{d}x = (8\kappa \cos\psi_i)^{-1}$ and $\mathrm{d}y = (8\kappa \sin\psi_i)^{-1}$, respectively. The time step used ranged from 0.157 to 0.196 which ensured that the Courant number was always less than one.

The numerical algorithm is verified by checking conservation of volume and energy for a solitary wave, where $a_i = 0.1$ and $\psi_i = 0°$. Figure 2(*a*) shows that the amplitude of the solitary wave does not change, indicating that energy is conserved. Table 1 shows that the greatest error for conservation of volume is $-0.0022\,\%$, which is likely caused by the initial condition given by the third-order solution; the error qualitatively presents itself as a formation of small trailing waves.

In certain trials (with $\psi_i = 10°$ and $15°$ for values of k close to unity) it is necessary to perform a translation on Φ^S and η due to the long propagation time. This translation is performed before the leading crest reaches the end of the domain. The translation is given by $\Phi^S_{new}(x, y, t) = \Phi^S(x - X_{new}, y, t)$ and $\eta_{new}(x, y, t) = \eta(x - X_{new}, y, t)$, where Φ^S_{new} and η_{new} are the translated values of the free surface velocity potential and surface displacement, respectively. This process is repeated in a cyclic manner until the simulation is terminated. The leading crest

https://doi.org/10.1017/jfm.2018.926 Published online by Cambridge University Press

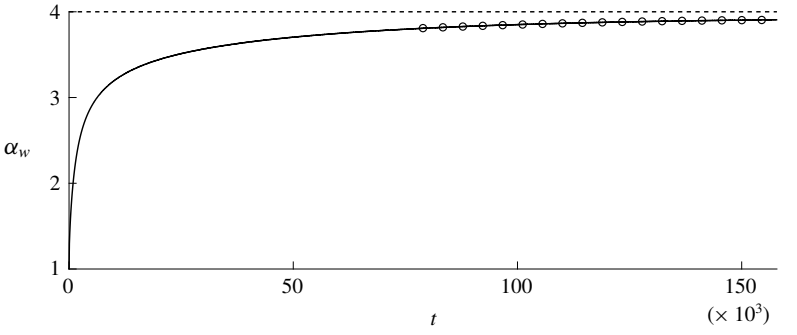


FIGURE 3. Evolution of amplitude for the case $a_i = 0.0108$, $k = 1.0$, $\psi_i = 10°$. The solid line is the amplification at the wall. The circles are the fit polynomial used to calculate that the slope at $t = 157\,860$ is 3.00×10^{-9}.

is extended in order to prevent the effects of diffraction along the offshore boundary from the wall. An overlay is presented in figure 2(*b*) for the case $a_i = 0.03$, $\psi_i = 15°$. The overlays are calculated by taking a cross section perpendicular to the crest in a region where the extension algorithm is being applied. The phase speed is also checked for this case and the maximum value of relative error between the measured phase speed and theoretical higher-order phase speed (Grimshaw 1971) is $-0.009\,\%$.

3. Results

Three different angles of incidence were examined ($\psi_i = 10°$, $15°$ and $26°$) for a range of interaction parameters ($0.5 \leqslant k \leqslant 1.31$). We also revisited the work of Tanaka (1993) by extending the simulation times for $a_i = 0.3$ with $\psi_i = 30°$, $35°$ and $40°$. Figure 3 is demonstrative of how small the growth rate had to be before terminating the simulation. The wave amplification is plotted against the interaction parameter k in figure 4, where the KP amplification $\hat{\alpha}$ is given by (1.3). An amplification of $\hat{\alpha} = 3.91$ is achieved when $\psi_i = 10°$ and $a_i = 0.0108$ ($k = 1.0$).

We also examine the length of the stem wave formation (see figure 1) for three different cases: ($\psi_i = 26°$, $k = 0.90$), ($\psi_i = 10°$, $k = 1.0$) and ($\psi_i = 15°$, $k = 1.01$). In the first case, the Mach stem length is continually growing even after the amplitude at the wall has reached an asymptotic state. For the latter two cases, the stem length has stopped growing by the time the amplitude at the wall has reached an asymptotic state. This observation of the numerical experiments is consistent with the theoretical prediction made by Miles (1977*a*,*b*) and, more explicitly, by Kodama & Yeh (2016).

The results by Funakoshi (1980) for $a_i = 0.05$ are also presented in figure 4(*a*). The good agreement seen in Funakoshi's results comes from the fact that he is solving equations that are on the same order of approximation as Miles's theory. Comparison of the solid and hollow triangle symbols in figure 4(*b*) demonstrates a clear improvement of the present data over Tanaka's, particularly for the $30°$ ($k = 0.789$) and $35°$ ($k = 1.024$) cases; this improvement is owing to the better computational hardware available to the present study.

When $k < 1$ a three-wave resonant interaction occurs. On the other hand, when $k > 1$ the KP solution is described as a simple reflection accompanied by a phase shift. When $k = 1$ there is a weak discontinuity-type singularity and the interaction is no longer clearly defined. After this point $k = 1^+$ the amplification begins to drop off sharply which appears to be in agreement with the numerical results.

https://doi.org/10.1017/jfm.2018.926 Published online by Cambridge University Press

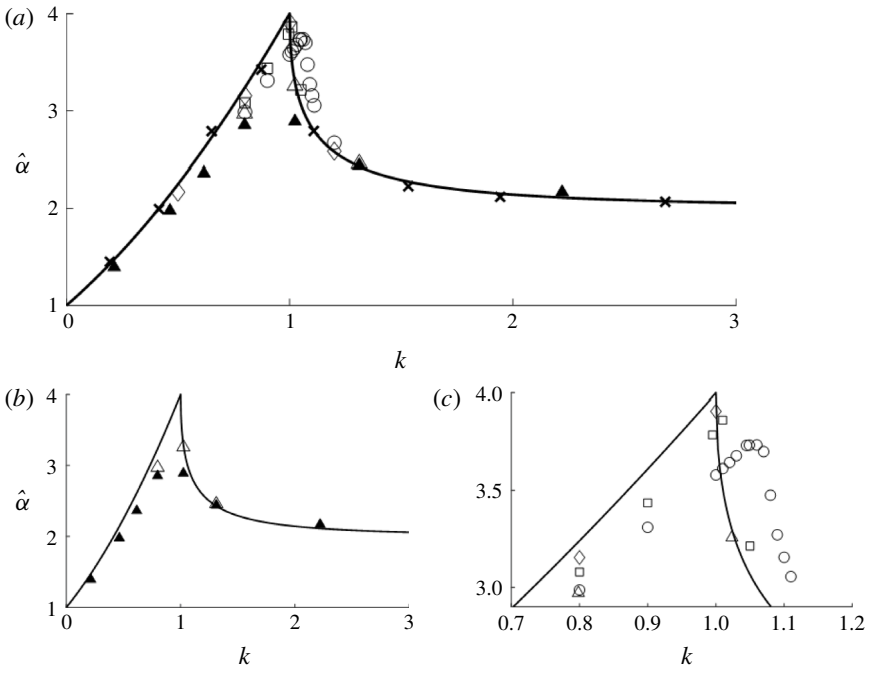


FIGURE 4. Amplification for several higher-order interaction parameters. The solid line is the theoretical curve, ▲ = Tanaka original, △ = Tanaka new, × = Funakoshi, ◇ = 10°, □ = 15°, ○ = 26°. (*a*) All the data; (*b*) comparison of Tanaka's data; (*c*) closeup view of data near $k = 1.0$.

After computing the amplification at various k values, we see that there is a dependency on ψ_i near $k \approx 1$ (figure 4*c*) and the data no longer agree well with the theoretical curve. These results show that $\hat{\alpha}$ shifts down and to the right as ψ_i increases. The open circle and open triangle overlap nicely for the data at $k = 0.8$ in figure 4(*c*). The angles used in these two different simulations were similar (open triangle: $\psi_i = 30°$; open circle: $\psi_i = 26°$). However, the nonlinearities used are considerably different (open triangle: $a_i = 0.3$; open circle: $a_i = 0.1$) indicating that the incident wave angle appears to have more of an impact on the amplification than the nonlinearity. At $k = 0.8$, we see that the amplification appears to increase monotonically as the angle of incidence is decreased.

4. Discussion

Note that in the results an amplification of 4 is nearly realized in one of the numerical simulations. The discrepancy between the numerical result of 3.91 and the theoretical fourfold amplification stems primarily from the ambiguity of the theory itself and the long simulation time for the numerical model to reach an asymptotic state. KP theory requires the angle of incidence to be small and, therefore, at the critical condition ($k = 1$) the nonlinearity must also be small. However, without a quantitative definition of 'small', it is difficult to determine what the angle and amplitude need to be in order to achieve the fourfold result. As seen in figure 4, the derivative is undefined at $k = 1$ and, therefore, it is not clear what will happen and it may take an even longer time to reach an asymptotic state if it even ever does reach

https://doi.org/10.1017/jfm.2018.926 Published online by Cambridge University Press

that limit in a finite amount of time. Therefore, the theory itself has some limitations even after the higher-order corrections presented in Kodama & Yeh (2016).

It takes a very long time (≈14 h of scaled physical time for the $h_0 = 1$ m case, for example) to reach an amplification of 3.91, which demonstrates that this particular result is of little practical significance. Therefore, we are unlikely to realize this result through physical laboratory experiments and even less likely to observe this result in the field.

5. Conclusions

The oblique incidence of solitary waves at a vertical wall were studied. A higher-order pseudo-spectral method was implemented in order to simulate experiments for $\psi_i = 10°$, 15° and 26° for various interaction parameters ($0.5 \leqslant k \leqslant 1.31$). We also re-computed the cases presented by Tanaka (1993), resulting in improvement after substantially extending the simulation time; the improvement was attributed to the advances in computational power achieved in the last 25 years. All results were then compared with the theoretical prediction of Miles (1977*b*) after converting the results to the higher-order KP theory given by Kodama & Yeh (2016). The greatest amplification achieved was $\hat{\alpha} = 3.91$ when $a_i = 0.0108$, $\psi_i = 10°$, almost realizing the fourfold prediction. It appeared that the amplification was sensitive to the angle of incidence when k was near unity. By performing these simulations with the full water-wave model, we have provided results which contribute to the quantitative validity of Miles's theory, at last.

REFERENCES

BOYCE, W. E. & DIPRIMA, R. C. 2009 *Elementary Differential Equations and Boundary Value Problems*, 9th edn. Wiley.

CHAKRAVARTY, S. & KODAMA, Y. 2009 Soliton solutions of the KP equation and application to shallow water waves. *Stud. Appl. Maths* **123** (1), 83–151.

CRAIG, W. & SULEM, C. 1993 Numerical simulation of gravity waves. *J. Comput. Phys.* **108** (1), 73–83.

DOMMERMUTH, D. G. & YUE, D. K. P. 1987 A high-order spectral method for the study of nonlinear gravity waves. *J. Fluid Mech.* **184**, 267–288.

FUNAKOSHI, M. 1980 Reflection of obliquely incident solitary waves. *J. Phys. Soc. Japan* **49** (6), 2371–2379.

GRIMSHAW, R. 1971 The solitary wave in water of variable depth. Part 2. *J. Fluid Mech.* **46** (3), 611–622.

JIA, Y. 2014 *Numerical Study of the KP Solitons and Higher Order Miles Theory of the Mach Reflection in Shallow Water*. The Ohio State University.

KODAMA, Y. & YEH, H. 2016 The KP theory and Mach reflection. *J. Fluid Mech.* **800**, 766–786.

LI, W., YEH, H. & KODAMA, Y. 2011 On the Mach reflection of a solitary wave: revisited. *J. Fluid Mech.* **672**, 326–357.

MELVILLE, W. K. 1980 On the Mach reflexion of a solitary wave. *J. Fluid Mech.* **98** (2), 285–297.

MILES, J. W. 1977*a* Obliquely interacting solitary waves. *J. Fluid Mech.* **79** (1), 157–169.

MILES, J. W. 1977*b* Resonantly interacting solitary waves. *J. Fluid Mech.* **79** (1), 171–179.

VON NEUMANN, J. 1943 Oblique reflection of shocks. *John von Neumann Collected Works* **6**, 238–299.

PERROUD, P. H. 1957 The solitary wave reflection along a straight vertical wall at oblique incidence. *Tech. Rep.* California Univ Berkeley Wave Research Lab.

TANAKA, M. 1993 Mach reflection of a large-amplitude solitary wave. *J. Fluid Mech.* **248**, 637–661.

ZAKHAROV, V. E. 1968 Stability of periodic waves of finite amplitude on the surface of a deep fluid. *J. Appl. Mech. Tech. Phys.* **9** (2), 190–194.

https://doi.org/10.1017/jfm.2018.926 Published online by Cambridge University Press